Journal of Non-Crystalline Solids 431 (2016) 140–144

Contents lists available at ScienceDirect

Journal of Non-Crystalline Solids

journal homepage: www.elsevier.com/locate/jnoncrysol

Optical and scintillation properties of Ce-doped $34Li_2O–5MgO–10Al_2O_3–51SiO_2$ glass

Takayuki Yanagida [a,*], Jumpei Ueda [b], Hirokazu Masai [c], Yutaka Fujimoto [a], Setsuhisa Tanabe [b]

[a] *Graduate School of Materials Science, Nara Institute of Science and Technology, 8916-5 Takayama-Cho, Ikoma, Nara 630-0192, Japan*
[b] *The Graduate School of Human and Environmental Studies, Kyoto Univ., Kyoto, Japan*
[c] *Institute for Chemical Research, Kyoto University, Uji, Kyoto, Japan*

ARTICLE INFO

Article history:
Received 10 December 2014
Received in revised form 8 April 2015
Accepted 19 April 2015
Available online 22 April 2015

Keywords:
Scintillator;
Li-glass;
Neutron;
Luminescence

ABSTRACT

Ce-doped $34Li_2O–5MgO–10Al_2O_3–51SiO_2$ glass was prepared by the conventional melt quenching method and compared with commercially available material, Li-glass (Saint Gobain) on their optical and scintillation properties. They exhibited 80% transmittance at wavelength longer than 350 nm. Photoluminescence (PL) emission peaks of the prepared glass and Li-glass resulted 385 and 420 nm, respectively. Temperature dependences of PL of these materials were examined from 25 to 300 K and they showed different responses. In X-ray induced scintillation spectra, emission peaks were similar to those in PL. Primary scintillation decay time of the prepared glass was largely faster than the conventional Li-glass and resulted few ns. In thermally stimulated luminescence glow curve, the prepared glass showed a deeper trap and it showed better afterglow property. Finally, ^{252}Cf neutron induced light yield was evaluated and the light yield of the prepared glass was around 10% of that of Li-glass.

1. Introduction

Scintillators are one of the luminescent materials which convert the absorbed energy of ionizing radiation (typical energy of KeV–GeV) to thousands of visible photons immediately via the energy migration from the host to emission centers [1]. Spectrum of applications of scintillators is quite wide such as medical [2], security [3], well-logging [4], and high energy physics [5]. Since the interaction between ionizing radiation and materials depends on kinds of ionizing radiation (photons or particles), many kinds of scintillators have been developed [6]. Recently, development of scintillators for thermal neutron detection attracts much attention due to the lack of ^{3}He gas [7–9]. The most conventional detector for thermal neutron detection has been ^{3}He gas proportional counters because ^{3}He has a high cross section against neutrons and low γ-ray sensitivity [9]. However, demands for ^{3}He gas have highly exceeded the supply capability so that any alternative detectors are highly required. One of the solutions to ^{3}He problem is a scintillation detector and many new scintillators for neutron detections are developed.

In the mid-20th century, some new inorganic scintillators for thermal neutron detection were introduced [10] and among them Li-glass scintillator (Saint Gobain) [11] was the most balanced one. Other scintillators have some disadvantages in practical applications. Eu-doped LiI had a huge hygroscopicity and was not easy in user handling. LiF–ZnS: Ag powder or sintered ceramic was translucent and thick samples could not be available so that high detection efficiency could not be achieved. On the other hand, Li-glass is non-hygroscopic and transparent thus many users prefer it. The weak point of Li-glass is its relatively slow scintillation decay. The activator ion is Ce^{3+} and it typically exhibits 70–100 ns scintillation decay [10,11]. To develop fast and efficient materials, some new scintillators like $LiCaAlF_6$ [12,13] and elpasolite [14,15] crystal scintillators were developed few years ago. To our knowledge, though many scintillators were invented, these two kinds became commercial products. Since many researchers concentrate to develop crystal scintillators, there is still a large room for study glass scintillators. Recently, fluoro-phosphate glass scintillator activated with Pr^{3+} was introduced and it was customized to observe scattering neutrons in nuclear fusion [16]. Though scintillation light yield of Pr-doped glass was not so high [16], it was sufficient only to observe very intense neutron emission in the nuclear fusion.

The aim of this study is to develop Ce^{3+}-doped glass scintillator with fast decay time. One of the disadvantages of above Pr-doped glass was a short emission wavelength in UV-C. Conventional photomultiplier tubes (PMTs) are developed to detect visible photons and generally quantum efficiency in UV wavelength is not so high. By this reason, most scintillator materials are activated with Ce^{3+} as an emission center. In addition, it has been reported that the presence of Ce^{4+} in the Ce^{3+}-doped scintillator, such as Lu_2SiO_5 [17] and $(Lu_{1-x}Y_x)_2SiO_5$ [18], enhanced the light yield and formed a new fast radiative recombination pathway. In this study, we prepared Ce^{3+}/Ce^{4+}-doped glass in air atmosphere and compared scintillator properties between Ce^{3+}-singly doped glass and Ce^{3+}/Ce^{4+}-doped glass.

---

* Corresponding author.
E-mail address: t-yanagida@ms.naist.jp (T. Yanagida).

http://dx.doi.org/10.1016/j.jnoncrysol.2015.04.033

2. Experimental procedures

Ce-doped $34Li_2O$–$5MgO$–$10Al_2O_3$–$51SiO_2$ glasses (in molar ratio) were prepared by the conventional melt quenching technique using CeO_2 (3N), Li_2CO_3 (4N), MgO (3N), Al_2O_3 (3N), and SiO_2 (3N) as starting materials. The batch was melted in a 50 cm^3 Pt crucible at 1400 °C for 1 h in air condition [19]. Hereafter we call the prepared glass ID1. Basically, chemical composition (cation molar ratio) of the ID1 was the same with that of Li-glass GS20 (Saint Gobain), but the preparation procedure was different.

Optical in-line transmittance was evaluated by using JASCO V670 spectrometer. Then, photoluminescence (PL) emission map and quantum yield (QY) were observed by Hamamatsu Quantaurus-QY. PL decay time profiles were evaluated with Hamamatsu Quantaurus-τ. The excitation wavelength was 280 nm and the monitoring wavelength was determined by emission maps. These optical characterizations were done at room temperature. In addition, temperature dependence of PL was investigated from 25 to 300 K with 25 K step. The setup of the PL temperature dependence was described previously [20]. Since Li-glass was one of the standard scintillators from the mid-20th century and there were many data on the temperature dependence (e.g., [21]), we focused on the temperature dependence of ID1.

X-ray induced scintillation spectra of samples were evaluated by using our original setup described previously [22]. Bias voltage and tube current of X-ray generator were 80 kV and 2 mA, respectively. Scintillation photons from samples were fed into optical fiber and then to monochromator equipped CCD detector (Andor iDUS420). By using pulse X-ray equipped streak camera system [23], we observed wavelength resolved scintillation decay time profiles. Monitoring wavelengths were the same in PL decay time evaluation. ^{252}Cf neutron induced pulse height spectra to determine scintillation light yield was carried out with our standard pulse height setup [24]. In pulse height characterization, shaping time was changed from 0.5 to 10 μs. Thermally stimulated luminescence (TSL) glow curves were evaluated by TL2000 (Nanogray) [25] after 1 Gy X-ray exposure. The heating rate was 1 K/s. Finally, X-ray induced afterglow profiles were investigated by afterglow characterization system [26].

3. Experimental results

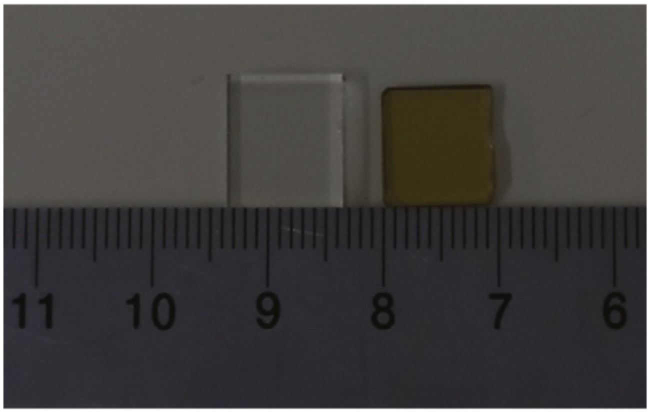

Fig. 1. Picture of Li-glass (left) and ID1 (right).

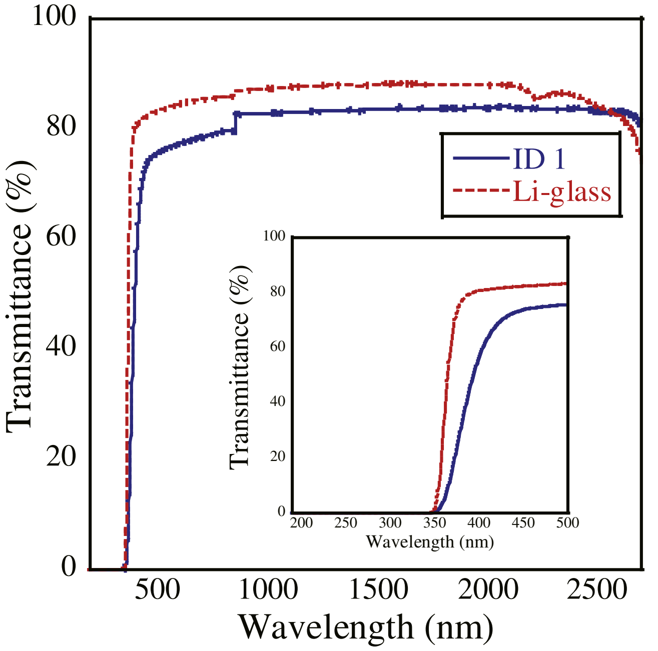

Fig. 2. In-line transmittance spectra of Li-glass and ID1.

Fig. 1 represents the ID1 and reference Li-glass (GS20) scintillators. While Li-glass was visibly transparent, the color of ID1 was brown. Then, Fig. 2 shows in-line transmittance of two samples. Optical transmittance was 70–80% at wavelength longer than 370 nm and transmittance of ID1 was slightly worse than the product in all wavelength. The absorption around 370 nm of ID1 was much stronger than Li-glass and it was consistent with their appearance. The absorption around 370 nm can be caused by the edge of charge transfer band from O^{2-} to Ce^{4+} [27], so that the ID1 glass contains more Ce^{4+} compared with the Li-glass (GS 20).

PL emission maps are shown in Fig. 3. PL emission peak wavelength of ID1 was around 420 nm while that of Li-glass was 385 nm under 320 nm excitation. PL quantum yields of ID1 and Li-glass were 2% and 90%, respectively. Emission wavelength of Li-glass was consistent with previous reports (e.g., [10]) and it showed quite high QY. On the other hand, emission wavelength of the ID1 was also typical value of Ce^{3+} 5d–4f transition in silicate glasses. The inset of Fig. 3 exemplifies PL emission spectrum of the ID1 and it has a broader bandwidth than that of Li-glass. By the temperature dependence of PL emission spectrum as shown in the inset of Fig. 4, the PL band is found to be composed of two Gaussian peaks centered at 390 and 420 nm. The energy difference between two peaks at 390 and 420 nm is 4000 cm^{-1}, which is larger than the typical energy difference between $^2F_{7/2}$ and $^2F_{5/2}$ of Ce^{3+} (2000–2800 cm^{-1} in LaF_3:Ce^{3+}). Therefore, two PL peaks can be attributed to the 5d–4f transition in different Ce^{3+} site. In Fig. 3, Li-glass shows that the PL peak wavelength is red-shifted by increasing excitation wavelength. This results show that this glass has many different environments around Ce^{3+} ions. Although the ID1 glass does not show the PL peak shifting by excitation wavelength clearly, it has the same glass composition to the Li-glass. Therefore, the ID1 glass could also have similar environment around Ce^{3+} ion to that in the Li-glass. These results also support that the two PL peaks are due to the variation of Ce^{3+} site. Fig. 4 shows relative PL intensities of these two peaks plotted against the temperature. PL intensity was an area of Gaussian fitting results and normalized to 1 at 25 K. The tendency of the PL intensity at 390 and 420 nm as a function of temperature is almost the same.

In Fig. 5, PL decay time profiles of ID1 and Li-glass are exhibited. The monitoring wavelengths of ID1 and Li-glass were their peak emission wavelength, 390 and 420 nm, respectively. PL decay time profiles of ID1 and Li-glass resulted 3 and 40 ns, respectively. The fast decay time of ID1 is due to the quenching by Ce^{4+} ions. In PL decay time profiles, no significant difference was observed in two emission peaks (390 and 420 nm) of ID1.